

Evolving Offshore Wind: A Genetic Algorithm-Based Support Structure Optimization Framework for Floating Wind Turbines

Matthew Hall, Brad Buckham, and Curran Crawford

Department of Mechanical Engineering, University of Victoria
Victoria, British Columbia, Canada

Abstract—This paper presents a genetic algorithm-based optimization framework for floating offshore wind turbine support structures. Using a nine-variable support structure parameterization, this framework spans a greater extent of the design space than preexisting optimization approaches in the literature. With a frequency-domain dynamics model that includes linearized hydrodynamic forces, linearized mooring forces, and linearized wind turbine effects, the framework provides a good treatment of the important physical considerations while still being computationally efficient. The genetic algorithm optimization approach provides a unique ability to visualize the design space. Application of the framework to a hypothetical scenario demonstrates the framework's effectiveness and identifies multiple local optima in the design space – some of conventional configurations and others more unusual. By optimizing to minimize both support structure cost and root-mean-square nacelle acceleration and plotting the design exploration in terms of these quantities, a Pareto front can be seen. Clear trends are visible in the designs as one moves along the front: designs with three outer cylinders are best below a cost of \$6M, designs with six outer cylinders are best above a cost of \$6M, and heave plate size increases with support structure cost. The complexity and unconventional configuration of the Pareto optimal designs may indicate a need for improvement in the framework's cost model.

I. INTRODUCTION

Interest in floating offshore wind turbines is accelerating rapidly, with a handful of MW-scale projects around the globe announced in the last year. Supporting wind turbines on floating platforms which are held in place by mooring lines allows wind turbines to be situated over waters hundreds of meters deep, vastly expanding the possibilities for offshore wind energy harvesting. Despite the recent surge in planned projects, great uncertainty remains as to the best support structure configuration on which to float a wind turbine. The world's first MW-scale prototype, Statoil's Hywind, uses a spar-buoy configuration of the type shown in Fig. 1(a). The world's second MW-scale prototype, Principal Power's WindFloat, uses a three-column semisubmersible platform of the type shown in Fig. 1(b). Other designers are putting their efforts behind a tension leg platform (TLP) configuration, such as is shown in Fig. 1(c).

The three illustrations in Fig. 1 represent the three stability classes that are used to group floating wind turbine support structures. Ballast-stabilized designs, such as the Hywind, use

ballast to lower the center of gravity below the center of buoyancy and tend to be of the spar-buoy configuration. Buoyancy-stabilized designs, such as the WindFloat, use a wide water plane area to raise the metacenter above the center of mass and are commonly of the multi-cylinder semisubmersible configuration. Mooring-stabilized designs, also known as tension leg platforms (TLPs), use well-spaced vertical mooring lines under significant tension against the platform buoyancy to submerge and stabilize the platform.

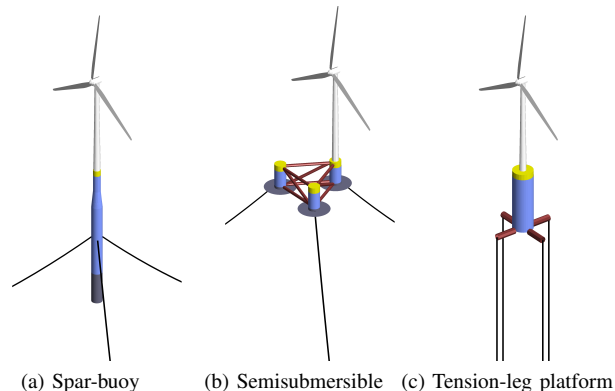


Fig. 1. Example floating wind turbine support structures

Despite the wide variety of support structure configurations being pursued and the complex tradeoffs between them, there is a surprising lack of published research aimed at exploring and comparing the full range of design options. One support structure optimization framework is WindOpt, created by Marintek for optimizing spar-buoy support structures [1]. It parameterizes the platform as a stack of four differently-sized cylinder sections with a damper plate on the bottom. The best example in the literature of a broad design space exploration is the parameter study done by Tracy [2]. This study's parameterization uses a cylindrical platform of variable dimensions and mooring lines of variable tension and angle – thereby spanning each stability class, from TLPs to spar-buoys to cylindrical barges – and frequency-domain modeling to find Pareto-optimal support platform configurations. Still, multi-cylinder configurations are excluded. Comparison studies considering multi-cylinder platforms have been done (eg. [3] and [4]). These are useful for examining the trade-offs between specific designs in detail, but they lack the ability to

explore the design space for new design concepts.

To provide a global optimization framework for the support structure, a parameterization that captures the full range of the design space is required. This means that the parameterization must be able to represent existing design geometries as well as feasible not-yet-conceived ones. Creating a scheme that meets those requirements is one challenge. A second challenge is integrating modelling techniques into a combined model that can evaluate the designs created by the scheme. A third challenge is creating the optimization framework that the scheme operates in; the many discontinuities in the design space (from different numbers of cylinders, different configurations, etc.) and potential for multiple competitive local optima require a special type of optimization algorithm.

An optimization framework that meets these challenges has been developed. It spans a greater extent of the design space than past support structure optimization attempts existing in the floating wind turbine literature [5], [1]. The framework has three components:

- 1) a support structure decision variable scheme that provides the parameterization to describe the design space (discussed in Section II),
- 2) a frequency-domain dynamics model to evaluate points in the design space (discussed in Section III), and
- 3) a genetic algorithm to manage the exploration of the design space (discussed in Section IV).

Each of these components was developed in sufficient depth in order to be able to demonstrate the operation of the overall framework, as is done in Section V. These results employ rough estimates of input parameters and cost functions in order to demonstrate the *potential* of the framework in the absence of more accurate input data.

The goal of the framework is not to automate the design process. Rather, the intention is to provide a framework that can be applied to a given siting scenario to produce a list of the most promising floating support structure configurations. These configurations can then serve as starting points for more detailed design processes. This way, more conventional design approaches (and optimizations) will converge to optimal designs faster, and promising design options will not be overlooked for lack of imagination. As well, application of the framework may provide insight into the nature of the design space.

II. SUPPORT STRUCTURE PARAMETERIZATION

The heart of the optimization framework is the support structure parameterization scheme. The scheme was made with the aim of describing the widest range of feasible platform and mooring system configurations with as few design variables as possible. It consists of components to deal with the platform geometry, the mooring line configuration, the size of structural elements connecting the platform cylinders and fairleads, the use of ballast, and the cost of the overall structure.

A. Platform Geometry

A scheme based on vertical cylinders was selected to parameterize the platform geometry in light of the range of

existing platform designs and the preference for cylindrical hulls for hydrodynamic, structural, and manufacturing reasons. The scheme consists of a central cylinder whose radius and draft are variable, with the additional control of a variable amount of taper near the water plane, as well as an array of three or more outer cylinders whose radius, draft, and distance from the center are collectively variable. The outer cylinders can feature circular heave plates of variable size at their bases. The tapered section of the central cylinder is set to occur from 1/4 draft to 1/8 draft. Fig. 2 illustrates the geometry scheme, before mooring lines, connective structural elements, and structure above the water plane are added. The eight design variables of the geometry scheme are provided in Table I.

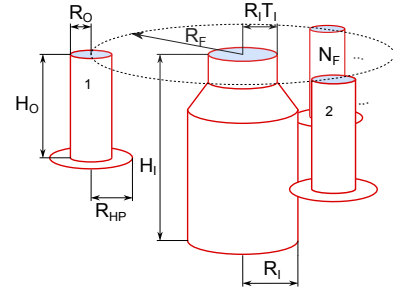


Fig. 2. Vertical cylinder-based platform geometry scheme

TABLE I. PLATFORM GEOMETRY SCHEME DESIGN VARIABLES

Variable	Description	Min.	Max.
H_I	inner cylinder draft	2 m	150 m
R_I	inner cylinder radius	3 m	25 m
T_I	inner cylinder top taper ratio	0.2	2
N_F	number of outer cylinders	3	6
R_F	radius of outer cylinder array	5 m	40 m
H_O	outer cylinders draft	3 m	50 m
R_O	outer cylinders radii	1.5 m	10 m
R_{HP}	outer cylinders heave plate radii	0 m	20 m

Constraints are applied to these variables to ensure that the cylinder diameter is not less than the tower base diameter (6 m [6]) and to avoid large taper angles near the water line.

Conditions are built into the geometry scheme to represent the various discontinuities that may arise. Inner or outer cylinder radii that are below the respective minimum bounds ($R_I < 3$ m or $R_O < 1.5$ m) signal that the respective cylinder(s) do not exist in the platform. Similarly, if the heave plate radius is less than the outer cylinder radius, heave plates are not considered in the analysis. Using these conditions allows the generic geometry parameterization shown in Fig. 2 to produce a wide range of platform configurations (see for example Fig. 12).

B. Mooring System

The mooring system scheme adds one more variable, x_M , to the design space. The mooring line configuration in the framework is then determined by this variable in conjunction with several of the platform geometry design variables and the water depth. The mooring scheme transitions smoothly between a taut vertical line configuration ($x_M \in [-1, 0]$), a taut catenary (non-vertical) line configuration ($x_M \in [0, 1]$), and a slack catenary configuration ($x_M \in [1, 2]$), as illustrated in Fig. 3. The number of mooring lines and the fairlead locations are determined by the platform geometry and x_M . This relatively

constrained setup was used to avoid wasting computation time on impractical mooring systems.

For single-cylinder designs with slack moorings, three lines are used, connected at half the cylinder draft. For single cylinder designs with taut moorings, four lines are used and they connect at the bottom of the cylinder. For multi-cylinder designs, a mooring line is connected at the outer edge of the bottom of each of the outer cylinders.

The anchor locations are determined by the mooring design variable and vary linearly with x_M from lying directly under the fairleads (when $x_M \leq 0$) to having a horizontal spread of double the water depth (at $x_M = 2$).

For slack mooring configurations, the unstretched mooring line length is determined according to

$$L_{unstr.} = \sqrt{l_x^2 + l_z^2} + \frac{l_z}{12} \quad (1)$$

where l_x is the horizontal distance from anchor to fairlead and l_z is the vertical distance from anchor to fairlead.

For taut configurations, the mooring line length is chosen such that the resulting line tension cancels any surplus buoyancy in the system (i.e. it is a function of the platform design variables) and no ballast in the platform is assumed. Taut vertical mooring configurations where the lines are held at a distance from the platform cylinder(s) by horizontal “tendons” (see Fig. 9(c)) are supported by negative values of x_M . The length of these tendons is then equal to $(-50m)x_M$.

The mooring line material properties are kept fixed, with elasticity modulus of 6 MPa and density of 12200 kg/m³. The mooring line cross-sectional area is varied inversely to the number of lines to keep the mooring system total mass proportional to the individual line length only. For three lines, the diameter is 90 mm, consistent with the OC3 Hywind design [7].

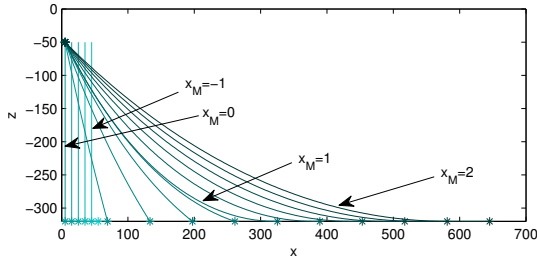


Fig. 3. Example mooring line profiles for $x_M \in [-1, 2]$

C. Taut-Mooring Tendon Arms

If a taut mooring configuration is used with tendon arms holding the fairleads at a distance radially from the platform, a scheme is needed to assign them realistic properties. These horizontal members are modelled as steel tubes with a constant wall thickness to radius ratio of $k = 5\%$. Their diameter is chosen for a bending moment criterion, based on the bending moment at the cylinder connection point. The load considered is the vertical component of the maximum steady-state mooring line tension multiplied by a safety factor of 3. This safety factor was chosen to calibrate the scheme to the

mooring specifications of the OC3 Hywind design. A yield stress for steel of $\sigma_y = 200$ MPa is used.

D. Float-Connecting Truss Members

If the platform features multiple cylinders, the structure connecting them together is an important contributor to the support structure dynamics and cost¹. In this framework, the structure connecting multiple hulls is modelled as a truss segment consisting of three tubular beams – two horizontal and one diagonal – between each pair of connected cylinders, as shown in Fig. 4. For platforms without an inner cylinder, adjacent cylinders are connected; for platforms with both inner and outer cylinders, each outer cylinder is connected to the inner cylinder. For strength, the truss section is kept quite tall, with the bottom member at 90% of the inner or outer cylinder draft (whichever is less) and the top member at a height of half the airgap above the waterline. The three members are treated

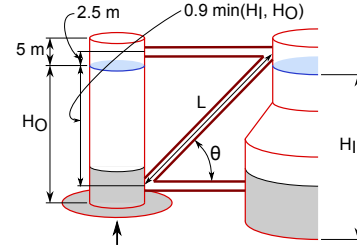


Fig. 4. Truss scheme for connecting cylinders

as hollow cylinders with a fixed wall thickness to radius ratio of 5%. The diameter of all three is chosen based on the pinned-pinned critical buckling load, P_{crit} , of the diagonal member:

$$P_{crit} = \frac{\pi^2 EI}{L^2} \quad (2)$$

where L is the length of the member, $E = 200$ GPa is the elasticity modulus of steel, and I is the tubular section’s moment of inertia. The compressive load, P , on this member is calculated based on a vertical load on the truss equal to the displaced weight of one of the outer cylinders, $\rho \nabla g$, or the maximum steady-state mooring tension, $T_{line max}$, if the mooring lines are connected to the outer cylinder, whichever is larger:

$$P = \frac{\max(\rho \nabla g, T_{line max})}{\sin(\theta)} \quad (3)$$

where θ is the angle of the diagonal member. A safety factor of 10 is applied to this vertical load; this value gives truss members diameters that are similar to those used in the OC4 WindFloat design [9].

E. Platform Mass and Ballast

The platform geometry scheme and mooring system scheme go hand-in-hand with a mass model that predicts the mass characteristics of the platform and determines the use of ballast. The mass of the main cylinders is modelled by assuming constant-thickness steel on their surface areas,

¹The high cost of such structures is what deters against platforms large enough to support multiple wind turbines. For an example of multi-turbine support structures, see [8].

including above the waterline. This thickness is greater than that of physical designs to also represent the mass of structural elements (bulkheads, stiffeners, stringers, etc.) within the platform. The other contributions to the platform mass come from the heave plates, the connective trusses and taut-mooring tendons, and the ballast. The ballast and connective structure are shown in Fig. 5.

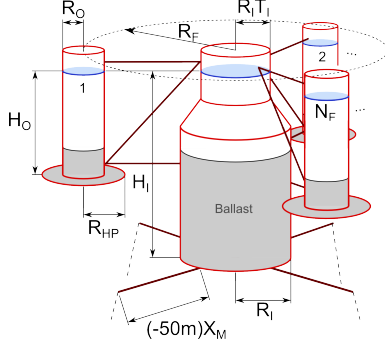


Fig. 5. Platform geometry scheme with ballast and connective structure

In the results here, the heave plate steel thickness is taken to be 30 mm and the hull steel thickness is determined by $T_{hull} = 50 \text{ mm} + 0.0003 \max(H_I, H_O)$ to account for the increased pressure forces at greater water depths. These values were selected in order to calibrate the scheme's mass model to be able to recreate the mass properties of the Hywind and WindFloat designs.

Once the mass of all the structural components is known, the amount of ballast is determined. The ballast mass is set according to the surplus buoyancy of the system – the remaining buoyancy force after subtracting wind turbine weight, platform structural weight, and the vertical component of mooring line tensions. In the case of taut mooring line configurations ($x_M < 1$), no ballast is applied and instead any surplus buoyancy is taken up by increasing the mooring system tension. In the case of slack mooring systems, ballast is added from the bottom of the deepest cylinder(s) upward, to a common top level across all cylinders. The contribution of the ballast to the distributed mass of the platform can then be calculated from these volumes.

The possibility of active ballast – pumping water ballast between cylinders to counter steady overturning moments – is also included for multi-cylinder designs. The effect is only considered in the analysis of the platform's static pitch angle; the shift in the platform center of mass is neglected in the dynamic analysis. For the static pitch angle calculation, the moment available from ballast shifting is modelled as

$$M = R_F \frac{N_F m_{ballast} O}{2} g \quad (4)$$

where $m_{ballast O}$ is the mass of ballast assigned to each outer cylinder (before shifting). This equation corresponds to shifting the ballast proportionally to the x -axis location of each cylinder (Fig. 6) and is a relation that holds true independent of the number of cylinders.

Concrete ballast with a density of 2400 kg/m^3 is assumed in order to enable ballast-stabilized designs. This is not necessarily incompatible with modelling buoyancy-stabilized designs

using water for active ballast, because the shallow draft of these designs makes their center of mass relatively insensitive to the ballast density.

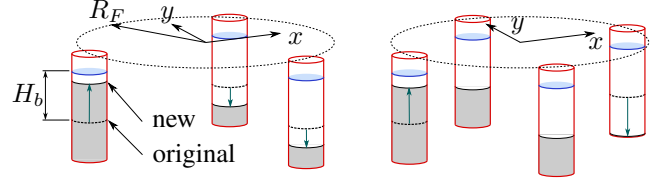


Fig. 6. Ballast shifting scheme

A certain amount of structure is needed above the waterline. Common freeboard or airgap heights range from 5 m in Tracy's parameter study [2] to 10 m in the WindFloat design [9]. A height of 5 m is used in the results generated here.

F. Support Structure Costs

The stability of a floating structure generally improves with structure size. The cost of the structure is the main factor that constrains this. As such, accounting for the support structure cost is crucial for a realistic representation of the design problem. The installed cost of the system is modelled as a combination of three component costs – for the floating platform, the mooring lines, and the anchors.

1) *Platform Structure*: The cost of the platform structure is treated as proportional to structure mass. This accounts for material costs as well as fabrication and installation costs in the simplest, linear way. Specific costs pertaining to different structural components are neglected. In a floating wind turbine platform study published with different cost numbers for different components, the per-mass cost differences between columns, trusses, braces, and deck differ by no more than 20% of the mean [10]. Considering the cost numbers of that study as well as the per-mass material and fabrication costs presented in [11], a cost of \$2.50 per kg of platform is used in the results here. Because of the inexpensive materials that can be used as ballast, a ballast cost is not used.

2) *Mooring Lines*: The cost of the mooring lines is treated as a linear function of their total combined length and the maximum steady-state tension they have to withstand. Implicit in this is the assumption that the peak tension the lines need to withstand will be proportional to the steady-state tension at the maximum wind speed condition. This is one of many approximations made to simplify the evaluation procedure of the framework. The line cost is based on a factor of \$0.42 /m-kN which is multiplied by the total line length and the maximum steady-state line tension. This gives final line cost results that fall within the range of costs spanned by [2], [10], [11].

3) *Anchors*: Anchor cost, for which installation cost is a significant component, is affected by both discrete anchor technology options and continuous anchor size factors. A three-technology anchor cost model was used in the framework to provide a simplified treatment of the anchor cost factors. The three anchor types considered in the framework are drag-embedment anchors, vertical-load drag-embedment anchors (VLAs), and suction piles. The cost of the anchors is modelled as a linear function of the maximum steady-state load on the

anchors. As with the mooring lines, the anchors are sized based on steady rather than peak loads because the latter would require a more involved iterative design approach. A fixed per-anchor installation cost is also included. Different cost coefficients are used for each type. The anchor type is chosen based on the angle of the mooring line at the anchor. The anchor cost coefficients and line angle criteria employed in the framework are given in table II.

TABLE II. ANCHOR COST MODEL

Anchor Technology	Line Angle	\$/anchor/kN (line tension)	\$/anchor (installation)
drag embedment	0°-10°	100	5000
vertical load (VLA)	10°-45°	120	8000
suction pile	45°-90°	150	11000

III. MODELLING AND EVALUATION METHODOLOGY

After the support structure decision scheme produces a design, the performance of the design needs to be evaluated. The evaluation of each point in the design space and calculation of its objective function value are handled by a six-DOF frequency-domain model created in Matlab. This linear model provides a computationally-efficient way of coupling the dynamics of the wind turbine, mooring system, and floating platform. Loads from steady winds and regular (monochromatic) waves are included. The DOFs considered are the six rigid-body modes of the platform. The frequency-domain equation of motion is

$$\{-\omega^2[M + A(\omega)] + i\omega[B(\omega) + B_{visc.}(\omega, \Xi)] + C\}\Xi(\omega) = Z(\omega)X(\omega)e^{i\omega t} \quad (5)$$

where Ξ is the 6-DOF complex response amplitude, M is system mass, A is hydrodynamic added mass, B is damping, $B_{visc.}$ is linearized viscous damping, C is stiffness, Z is wave amplitude, X is wave excitation coefficient, and ω is wave frequency. It is worth noting that the linearization inherent in $B_{visc.}$ is dependent on the response amplitude.

The complex response amplitudes, $\Xi(\omega)$, can then be solved for if the coefficients are known. The frequency-dependent response for unit amplitude waves, in terms of DOF amplitudes and phases, is commonly referred to as a response amplitude operator (RAO), where

$$RAO_i(\omega) = \Xi_i(\omega)/Z(\omega). \quad (6)$$

By definition, the frequency-domain model assumes that the platform motions are at the same frequency as the incident waves and that the incident waves are regular. While this means that the transient response of the system cannot be modelled, the assumption of linearity implies that the responses at different wave frequencies can be superimposed according to a wave spectrum to predict the system behaviour in irregular sea states.

A. Platform Hydrodynamics

For the hydrodynamics of the platform, linear hydrodynamic coefficients calculated by WAMIT are supplemented with linearized coefficients for the viscous drag forces on the platform cylinders, truss and tendon members, and heave plates. The linearization of these viscous drag terms is done iteratively during the equation-of-motion solution because the linearized terms are amplitude-dependent.

1) *Linear Hydrodynamics*: To calculate the linear hydrodynamic loads on the platform, the required linear hydrodynamic coefficients are generated for each platform design by the panel method code WAMIT. Before WAMIT is called, a meshing routine created in C++ discretizes the surface of each candidate platform design, including the heave plates, and generates the WAMIT geometry file. The same C++ routine also performs the platform mass calculations and handles the calls to the mooring line model. This process is embodied in a DLL and interfaced to Matlab using a .mex file. The interface returns a variety of aggregate platform properties to the Matlab-based frequency-domain model of the combined system.

2) *Heave Plate Viscous Drag*: The viscous drag of the heave plates, which is quadratic in nature and not related to wave radiation damping, is not modelled by WAMIT's linear potential flow method so another model is required to capture it. A linearization of the viscous drag term from Morison's equation is used [12]:

$$F(t) = \frac{2}{3}\rho D^3\omega B'u(t) \quad (7)$$

where D is heave plate diameter, $u(t)$ is the normal component of the relative fluid velocity, and B' is a function of Keulegan-Carpenter number for which empirical relations exist. Wave kinematics are not included in the calculation of relative fluid velocity for simplicity, on the grounds that heave plates are at a depth where wave velocities are quite low. The model provides the viscous drag contribution to the platform damping in the three DOFs most affected by the heave plates – heave, pitch, and roll. The wave-radiation damping and added mass from the heave plates are provided by the WAMIT analysis.

3) *Platform Viscous Drag*: A viscous drag model was also implemented for the platform cylinders, since the damping forces on slender cylinders are not adequately accounted for by a linear hydrodynamics approach alone. For these elements, a linearization of the drag term of Morison's equation is used, with a constant drag coefficient of 0.6 [13], [14]:

$$F_{drag,lin.} = \sqrt{\frac{8}{\pi}}\sigma_u \frac{1}{2}\rho d C_D u \quad (8)$$

where σ_u denotes the standard deviation or root-mean-square of u . As was done with the heave plate damping, wave kinematics are neglected and only the structure motions are used in the calculation of velocity; this simplifies the linear frequency-domain representation of the problem.

4) *Connective Element Added Mass and Drag*: To avoid the complexity of having to create a panel mesh for the connective trusses and tendons, and because the slenderness of these components makes their wave-radiation contributions relatively small, the trusses and tendons are not included in the WAMIT analysis. Rather, their hydrodynamic properties are accounted for by the viscous drag linearization already mentioned, and an added mass calculation of the form used in Morison's equation. The added mass coefficient used is 0.97 and the damping coefficient is 0.6 – these are the same coefficients as were used in the OC3 Phase IV modelling and in the modelling of the original Hywind design [15].

B. Wind Turbine

A linear representation of the NREL 5 MW offshore reference wind turbine [6] is used, with linearized coefficients obtained using FAST's linearization functionality for each wind speed condition. To limit the complexity of the model, these linearizations are generated at a fixed static pitch angle rather than one that is adjusted for each platform at the thrust load of each wind speed. A value of zero pitch was chosen because many platforms pitch very little or use techniques such as active ballast to eliminate significant static pitch angles.

C. Mooring Lines

The generation of mooring line stiffness matrices is handled by a C++ routine that calls a quasi-static mooring line model – in this case, a C++ translation of Catenary, the mooring line subroutine of FAST. The linearization routine uses several layers of iterations and perturbations to obtain linearized mooring stiffness matrices for the static surge displacements corresponding to the wind speeds being considered.

IV. GENETIC ALGORITHM OPTIMIZER

A genetic algorithm (GA) optimizer was selected as the most flexible and straightforward way to programmatically explore the design space, given the potential for multiple local optima and the diverse, interrelated, and often-discontinuous design variables. A pure gradient-based approach across the full configurational design space would be defeated by the discontinuities present. The GA provides clusters of designs around locally-optimal configurations, which is more useful than a single optimal design at this level of model fidelity for gaining insight into the characteristics of the design space.

A. Cumulative Multi-Niching Genetic Algorithm

The algorithm developed specifically for this framework, the Cumulative Multi-Niching (CMN) GA, has two goals that are not common to all GAs: to use as few objective function evaluations as possible and to be able to identify and converge to multiple local optima. Because the evaluation of each individual design (and the hydrodynamic analysis in particular) is vastly more time consuming than the operations of the GA itself, the algorithm has features designed to limit redundant or unproductive objective function evaluations. With the possibility of multiple local optima in the design space, the algorithm is also designed to support multi-niching - the ability to converge to multiple optima simultaneously. Recognizing that the limited fidelity of a frequency-domain model may create distortions in the design space and that additional factors not included in the framework also affect the choice of optimal design, the algorithm was developed to explore local optima in an equitable way, regardless of the comparative fitness values of the local optima, so that potentially promising configurations are not discriminated against based on potential deficiencies in the submodels.

One of the most distinctive features of the CMN GA is that it is cumulative; each successive generation adds to the overall population. By never discarding individuals from the population, the GA can make use of the information from every objective function evaluation as it explores the design space. This makes for a large population, which enables visualization

of the design space. An example population on a contrived two-dimensional design space is shown in Fig. 7. Performance demonstrations and a more thorough description of the CMN GA can be found in [16].

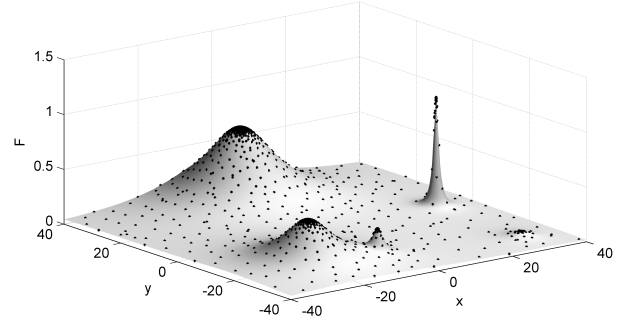


Fig. 7. Design space exploration of the CMN GA on a sample two-variable objective function (function F4 in [16])

B. Optimization Objectives

While minimizing cost of energy (COE) is the overall optimization goal for a renewable energy technology, a simpler optimization problem formulation can be used for the floating wind turbine support structure design problem, in order to avoid the additional considerations of modelling energy yield over the system's lifetime. In a floating wind turbine, large platform motions can potentially reduce turbine lifetime or reduce energy production. To account for this, minimization of platform motions that cause problematic turbine loadings is used as an optimization objective. The metric for the platform motions that affect the wind turbine is the root-mean-square (RMS) fore-aft nacelle acceleration [11], calculated as

$$\sigma_{a\,nac.} = \sqrt{\int_0^{\infty} |RAO_{a\,nac.}(\omega)|^2 S(\omega) d\omega} \quad (9)$$

where $S(\omega)$ is the power spectral density of the incident waves and

$$RAO_{a\,nac.}(\omega) = -\omega^2 [RAO_1(\omega) + z_{nac.} RAO_5(\omega)]. \quad (10)$$

The numerical subscripts denote the platform degrees of freedom (DOFs) – 1 being surge and 5 being pitch – and $z_{nac.}$ is the hub height of the turbine. This relates to the flapwise bending moments at the blade roots, which can be the most critical load in a wind turbine with a floating base. The other factor affecting COE is the support structure cost. It can either be capped or be minimized for in a multi-objective optimization², as in

$$\min J = W_1 \sum_{i=1}^n w_i (\sigma_{a\,nac.})_i + W_2 Cost \quad (11)$$

where w is a weighting function for the n metocean conditions evaluated, with $\sum w = 1$, and W_i is a weighting factor in the range $[0, 1]$ that controls the weighting between RMS nacelle

²Unlike cost, which is calculated before the hydrodynamic analysis, the platform motion is always treated as an objective rather than a constraint because its calculation requires full evaluation of the design in the frequency-domain model. This makes the design space exploration more computationally efficient.

acceleration and cost, with $\sum W = 1$. By considering turbine motion and support structure cost, the support structure design factors that are relevant for the COE of a floating offshore wind turbine are accounted for.

C. Constraints

In addition to the basic geometric constraints included in the design parameterization discussed in Section II, a number of performance constraints are applied to ensure candidate designs are feasible.

1) *Costs*: Total support structure cost as calculated according to the functions of Section II-F is capped at \$9M.

2) *Static Pitch Angle*: A limit of 10° is placed on the static pitch angle of the platform. This is a widely-used limit for floating wind turbines [10], [2], [11]. The static pitch angle, $\bar{\xi}_5$, is a function of the platform volume and center of buoyancy, the turbine and platform masses and centers of masses, the water plane moment of inertia, and the mooring system stiffness:

$$\bar{\xi}_5 = \frac{F_{thrust}z_{nac} + F_{l5} - \frac{1}{2}R_F N_F m_{ballast} O g}{\rho g \nabla z_{CB} - M g z_{CM} + \rho g I_{xx} - C_{5,5} + C_{5,1} z_{fair}} < 10^\circ \quad (12)$$

where F_{thrust} is the thrust loading on the turbine, F_{l5} is the force in the pitch DOF exerted by the mooring system at the maximum-thrust equilibrium surge displacement, ρ is water density, ∇ is platform displacement, z_{CB} is the center of buoyancy location, M is the total system mass, z_{CM} is the center of mass location, I_{xx} is the platform water plane moment of inertia in the pitch direction, $C_{l5,5}$ is the stiffness in pitch from the mooring lines, and $C_{l5,1}z_{fair}$ is the product of pitch-surge mooring stiffness and fairlead depth. This constraint is evaluated at the maximum wind thrust condition. For the NREL 5 MW reference turbine, this is 800 kN, and the hub height is 90 m [6]. The mooring system properties – F_{l5} , $C_{l5,5}$, and $C_{l5,1}z_{fair}$ – are based on the corresponding surge displacement. Equation (12), like the rest of the model, assumes small angles.

3) *Dynamic Pitch Angle*: A dynamic pitch constraint is necessary to ensure operating angle limits for the turbine and floating platform are not exceeded. Following the approach of Tracy [2], a maximum steady plus RMS pitch angle of 10 degrees is used:

$$\bar{\xi}_5 + \sigma_{\xi_5} < 10^\circ. \quad (13)$$

The standard deviation in pitch, σ_{ξ_5} , is calculated based on the wave spectrum and the platform's pitch RAO, similarly to (9).

4) *Slackness in Mooring Lines*: Snap loads, where a taut mooring line goes slack and then abruptly regains tension, can cause large loads and structural failure for taut-moored support structures. Avoiding taut lines going slack is therefore a design constraint. Using the frequency-domain approach, the potential for the mooring lines going slack is calculated using RAOs for the mooring lines using the same RMS approach as for the pitching motions.

$$\bar{T}_{line} - 3\sigma_{T_{line}} > 0 \quad (14)$$

where \bar{T}_{line} is the steady-state line tension and $\sigma_{T_{line}}$ is the RMS line tension variation about the mean calculated from the line tension RAO.

D. Inputs

The framework takes a number of inputs that characterize the operating environment of the floating wind turbine. These inputs are: water depth, a set of wave spectra, and a set of corresponding steady wind speeds. The site conditions would also have implications for the costs associated with the structure, and anchor costs in particular. In addition to these site-specific inputs, a number of inputs relating to design assumptions and constraints are used. As has been discussed previously, these include the type of ballast to be used, the expected hull thicknesses, the thicknesses of mooring cables, upper limits on the structural mass and mooring line tensions to reflect cost constraints, maximum acceptable static pitch angles, etc. All of these inputs reflect the nature of the framework as a global optimizer; once an operating environment and common design constraints are provided, the framework will explore all the options within those inputs according to its abilities.

The site-specific input variables used for the results presented here are a water depth of 300 m, wind speeds of 8 m/s and 12 m/s, and corresponding sea states of 5 m and 8 m significant wave heights, and 6 s and 10 s peak periods. The two environmental conditions are given equal weighting; the objective function is the average of the objective function value calculated for each of the two environmental conditions. The frequency range used in the analysis is from 0.25 rad/s to 2 rad/s, in 0.125 rad/s increments. The bottom of this range is below the wave excitation spectrum and the top of this range is above the active frequencies in typical RAOs.

V. RESULTS

This section presents optimization results generated by the framework using the input parameters described previously, in order to demonstrate the framework's operation and illustrate the design space described by the framework's parameterization.

A. Single-Cylinder Single-Objective Optimization

One of the simplest demonstrations of the framework's operation can be made by considering a single-cylinder design space. The four variables describing this design space are draft, H_I , radius, R_I , taper ratio, T_I , and mooring configuration, x_M . The three-dimensional scatter plot of Fig. 8 shows the framework's exploration of this design space in terms of H_I , R_I , and x_M , with a population size of 1500. The points evaluated by the GA can be seen to cluster around three configurations: spar-buoys on the right, wide ballasted cylinders on the left, and TLPs of various dimensions on the bottom. This demonstrates the framework's ability converge to multiple local optima, and shows that there are multiple local optima even in just the single-cylinder design space.

The five locally-optimal designs identified in Fig. 8 are illustrated in Fig. 9. The first locally-optimal design is a conventional spar buoy with a draft of 132 m and a diameter of 11.8 m. The second locally-optimal design is a large cylinder with 31700 tonnes of ballast (compared to 9900 tonnes for the spar-buoy), resulting in triple the displaced volume of the spar-buoy. This unconventional and massive design suggests that the structural cost model in the framework may need refinement.

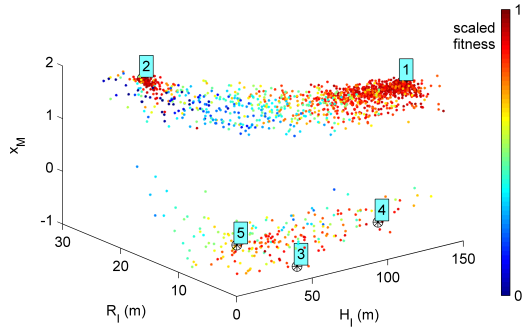


Fig. 8. Single-cylinder single-objective design space exploration

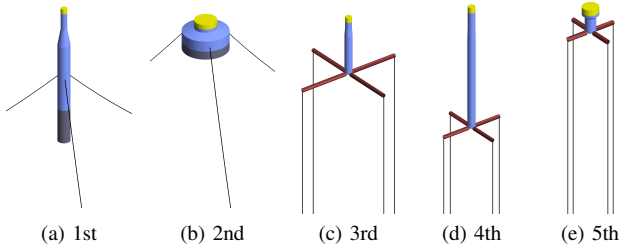


Fig. 9. Single-cylinder single-objective local optima

The next three locally-optimal designs are vertical-line TLPs with varying dimensions.

B. Single-Cylinder Multi-Objective Optimization

Changing from a single-objective nacelle-acceleration optimization to a weighted sum of both nacelle acceleration and cost and selecting appropriate weightings causes the GA to converge toward lower-cost designs. Combining the populations from three simulations with different weightings results in a more expansive exploration of the design space (Fig. 10). Each multi-objective optimization run was terminated once the design population reached 1000. Plotting these populations in terms of cost and nacelle acceleration reveals the presence of a Pareto front along the lower-left boundary of the cluster of points, as can be seen along with design illustrations in Fig. 11.

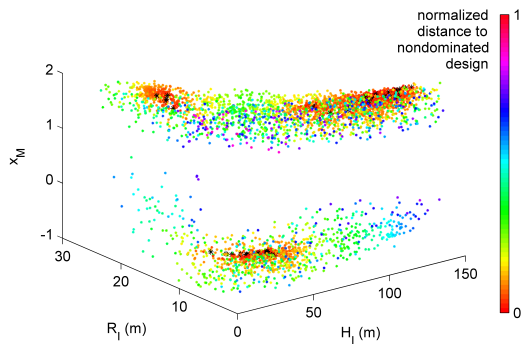


Fig. 10. Single cylinder multi-objective design space explorations

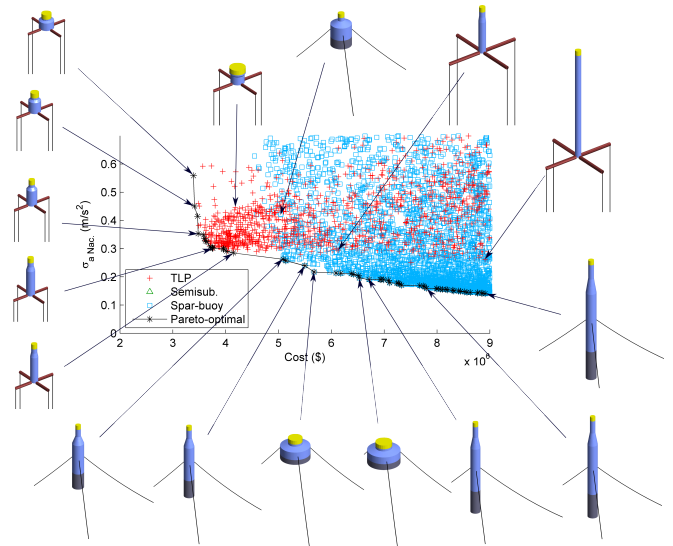


Fig. 11. Single-cylinder multi-objective performance space

As can be seen from Fig. 11, the spar buoy configuration is the most stable above a platform cost of about \$5M. Within that range, the large ballasted cylinder designs are competitive with more conventional spar-buoys for costs around \$5M to \$7M. Below \$5M, a TLP configuration can achieve greater stability for a given cost but cannot achieve as low accelerations as the higher-cost spar-buoys. No buoyancy-stabilized (barge-type) platform designs are to be seen on the single-cylinder Pareto front. There is a consistent trend along the entire Pareto front of deeper and narrower platforms as the cost increases. There is little variation in the mooring system, with $x_M \in [1.8, 1.95]$ above \$5M and $x_M \in [-0.4, -0.3]$ below \$5M.

C. Full Design Space Multi-Objective Optimization

Resolving a Pareto front for the full design space requires a larger number of objective function weightings than for the single-cylinder design space. This is because the possibilities for different numbers of cylinders and different mooring systems create many different niches for the GA to explore. These niches inhibit the GA from exploring a wide span of the Pareto front in a single optimization run of a given weighting. Seven weightings (detailed in Table III) are used, with a population size of 1500 in the optimization for each weighting.

TABLE III. FULL DESIGN SPACE OBJECTIVE WEIGHTINGS

	Run 1	Run 2	Run 3	Run 4	Run 5	Run 6	Run 7
W_1	1	1	1	1	1	1	1
W_2	0	2E-09	5E-09	2.5E-08	5E-08	1.5E-07	3E-07

A visualization of the framework's exploration, in a three-dimensional projection of the design space with axes for R_I , R_O , and x_M , is shown in Fig. 13. Two main clusters of designs are visible. One cluster is on the $R_I = 0$ plane, indicating designs that do not have a central cylinder. It should be remembered that the evaluated designs are not as similar as they look from the figure, because the other six design space dimensions are collapsed to produce the three-dimensional plot. The Pareto front and design illustrations are shown in the performance space plot of Fig 12.

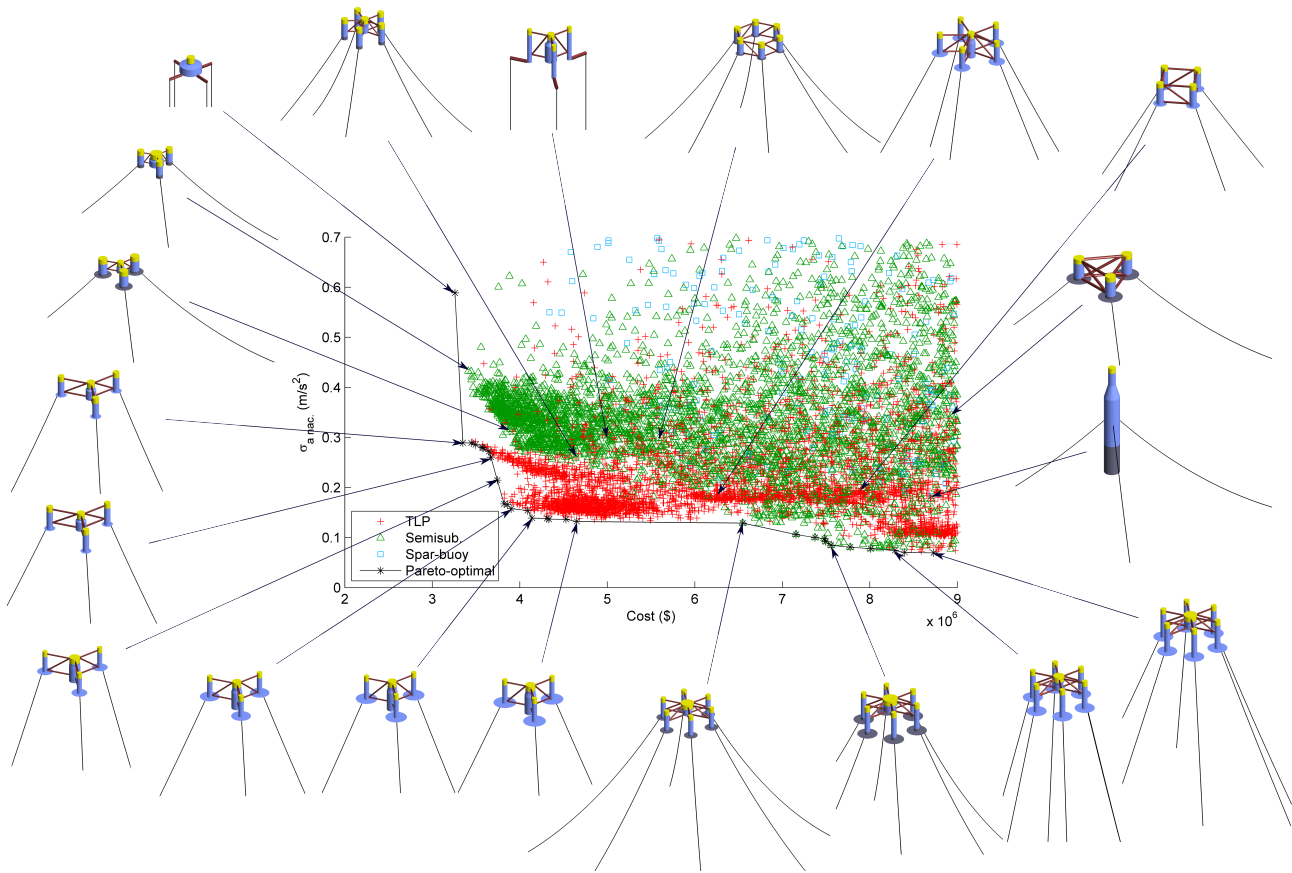


Fig. 12. Full multi-objective performance space

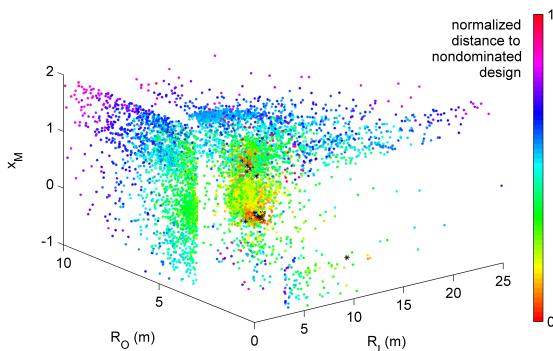


Fig. 13. Full multi-objective design space explorations

Above a cost of \$6M, the Pareto-optimal platform configurations feature six slender outer cylinders arrayed around a shorter central cylinder. Heave plates are used in all cases. The mooring system transitions from a taut system with non-vertical lines to a slack system as cost decreases, with ballast added to compensate. Heave plate size reduces as cost decreases.

Below a cost of \$6M, the Pareto-optimal platform configurations feature three slender cylinders arrayed around a central cylinder of similar draft but larger radius. The mooring system is taut but non-vertical, and the cylinder spacing can be seen to increase slightly, while the heave plate size decreases, as cost

decreases. It seems that cylinder spacing is more economical but less effective than heave plate area at reducing nacelle acceleration.

The lowest-cost non-dominated design departs from the others in being a single-cylinder shallow-draft TLP design. Its wide platform shape provides a very low surface area to volume ratio. It would seem that mooring line tension is the most economical way of stabilizing such a platform. Based on the costs, constraints, and environmental conditions specified for these results, it seems that there is little chance of feasible support structures costing less than \$3.4M.

VI. CONCLUSIONS

A global optimization framework has been developed for the floating wind turbine support structure design problem. A platform geometry scheme based on arrays of vertical cylinders and a mooring configuration scheme with one dedicated design variable provide a flexible and efficient means of describing a wide range of support structure configurations. A frequency-domain model evaluates the support structure performance in terms of platform motions in six degrees of freedom. A genetic algorithm controls the exploration of the design space, seeking local optima that minimize RMS nacelle acceleration and cost, which together constitute the most relevant support structure design factors affecting the cost of energy from a floating wind turbine.

Results produced from the framework using hypothetical

input data demonstrate the capabilities of the framework and reveal various characteristics of the design space. The framework converges reliably to locally-optimal designs. Some of these designs are conventional, such as the single-cylinder global optimum pictured in Fig. 9(a). In the full design space, however, the framework finds that less conventional configurations featuring multiple cylinders perform better. These designs feature a central cylinder surrounded by three or six outer cylinders equipped with heave plates, and often have taut non-vertical mooring lines. Surrounding these locally-optimal points in the design space are large swaths of feasible space. The GA approach of the framework is able to map these regions, allowing visualization of the nature of the design space – including the bounds imposed by expense, buoyancy, or stability constraints; the general effects of different parameters on the support structure’s performance; and the presence of multiple local optima.

By viewing the results in terms of both RMS nacelle acceleration and cost objectives, a Pareto front can be observed. Clear trends are visible in the designs as one moves along the front: three outer cylinders are best below a cost of \$6M, six outer cylinders are best above a cost of \$6M, and heave plate size increases with support structure cost. With the current settings, there appears to be a floor on support structure cost at around \$3.4M. At no point does a spar-buoy design sit on the Pareto front. The presence of these relatively complex four- and seven-cylinder platforms on the Pareto front, and the absence of simpler buoyancy- or ballast-stabilized designs, would appear to challenge the conventional wisdom in support structure design for floating wind turbines. However, the complexity of these designs may carry additional costs and risks not accounted for in the framework. If accounted for, these factors could tip the balance back toward more conventional single- or three-cylinder platform designs.

VII. FUTURE WORK

Further development of the optimization framework could be carried out in several areas. One area for improvement is in expanding the cost model to better account for the additional costs associated with more complex platform designs.

Another area for improvement is in the framework’s design evaluation process: improving the coupling between static pitch angle, wind turbine linearization point, and mooring system linearization point; and improving the sizing algorithms of structural elements and mooring lines to better reflect the dynamic loads they will face. These changes would require a more iterative design evaluation approach, in which the dynamics results feed back into the sizing of the structure components until a well-sized design is converged upon.

A third area of improvement lies in expanding the support structure parameterization to include a greater variety of design possibilities. It is challenging to develop flexible parameterizations that maintain order in the design space, but there may be potential for alternative approaches that do not rely on cylindrical geometries. As well, increased intelligence in the use of advanced features such as active ballast and different mooring line options could further expand the design space.

REFERENCES

- [1] I. Fylling and P. A. Berthelsen, “WINDOPT: an optimization tool for floating support structures for deep water wind turbines,” in *Proceedings of the ASME 2011 30th International Conference on Ocean, Offshore and Arctic Engineering*, Jan. 2011, pp. 767–776.
- [2] C. C. Tracy, “Parametric design of floating wind turbines,” M.Sc. Thesis, MIT, 2007.
- [3] J. M. Jonkman and D. Matha, “Dynamics of offshore floating wind turbines—analysis of three concepts,” *Wind Energy*, vol. 14, no. 4, pp. 557–569, May 2011.
- [4] A. Robertson and J. Jonkman, “Loads analysis of several offshore floating wind turbine concepts,” in *Proceedings of the Twenty-first International Offshore and Polar Engineering Conference*, Maui, Hawaii, USA, 2011.
- [5] P. Sclavounos, C. Tracy, and S. Lee, “Floating offshore wind turbines: Responses in a seastate pareto optimal designs and economic assessment,” Oct. 2007. [Online]. Available: http://web.mit.edu/flowlab/pdf/Floating_Offshore_Wind_Turbines.pdf
- [6] J. M. Jonkman, S. Butterfield, W. Musial, and G. Scott, “Definition of a 5-MW reference wind turbine for offshore system development,” National Renewable Energy Laboratory, Golden, Colorado, Tech. Rep. 38060, Feb. 2009.
- [7] J. Jonkman and W. Musial, “Offshore code comparison collaboration (OC3) for IEA task 23 offshore wind technology and deployment,” National Renewable Energy Laboratory, Golden, Colorado, Tech. Rep. 48191, Dec. 2010.
- [8] A. R. Henderson, R. Leutz, and T. Fujii, “Potential for floating offshore wind energy in japanese waters,” in *Proceedings of The Twelfth (2002) International Offshore and Polar Engineering Conference*, 2002, p. 26–31.
- [9] D. Roddier, A. Peiffer, J. Weinstein, and A. Aubault, “A generic 5MW WindFloat for numerical tool validation & comparison against a generic 5MW spar,” in *Proceedings of the ASME 2011 30th International Conference on Ocean, Offshore and Arctic Engineering*, Rotterdam, The Netherlands, Jun. 2011.
- [10] Bulder, van Hees, Henderson, Huijsmans, Pierik, Snijders, Wignants, and Wolf, “Studie naar haalbaarheid van en randvoorwaarden voor drijvende offshore wwindturbines,” Tech. Rep., Dec. 2002.
- [11] E. Wayman, “Coupled dynamics and economic analysis of floating wind turbine systems,” Ph.D. dissertation, MIT, May 2006.
- [12] L. Tao and D. Dray, “Hydrodynamic performance of solid and porous heave plates,” *Ocean Engineering*, vol. 35, no. 10, pp. 1006–1014, Jul. 2008.
- [13] L. E. Borgman, “Random hydrodynamic forces on objects,” *The Annals of Mathematical Statistics*, vol. 38, no. 1, p. 37–51, 1967.
- [14] F. Savenije and J. Peeringa, “Aero-elastic simulation of offshore wind turbines in the frequency domain,” Energy Research Center of the Netherlands, Tech. Rep., 2009. [Online]. Available: <ftp://nrg-nl.com/pub/www/library/report/2009/e09060.pdf>
- [15] L. Savenije, “Modeling the dynamics of a spar-type floating offshore wind turbine,” Ph.D. dissertation, Technical University Delft, 2009.
- [16] M. Hall, “A cumulative Multi-Niching genetic algorithm for multimodal function optimization,” *International Journal of Advanced Research in Artificial Intelligence*, vol. 1, no. 9, Dec. 2012.